Journal of Fluorescence, Vol. 10, No. 2, 2000

Mechanisms of Fluorescence Quenching in Donor–Acceptor Labeled Antibody–Antigen Conjugates

Uwe Schobel,[1] Hans-Joachim Egelhaaf,[1] Dieter Fröhlich,[1] Andreas Brecht,[2] Dieter Oelkrug,[1] and Günter Gauglitz[1,3]

Received September 28, 1999; accepted December 22, 1999

The cyanine dyes Cy5 and Cy5.5 are presented as a new long wavelength-excitable donor–acceptor dye pair for homogeneous fluoroimmunoassays. The deactivation pathways responsible for the quenching of the fluorescence of the antibody-bound donor are elucidated. Upon binding of the donor dye to the antibodies at low dye/protein ratios, its fluorescence quantum yield rises to unity. Higher dye/protein ratios lead to progressive aggregation of the dyes, which results in quenching of monomer fluorescence due to resonance energy transfer (RET) from the monomers to the nonfluorescent dimers. The dependence of the quenching efficiency on the labeling ratio is described quantitatively by assuming a Poisson distribution of the dyes over the antibodies. The maximum fluorescence intensity per antibody is obtained at a labeling ratio of 4. Upon formation of the antibody–antigen complex, electron transfer and RET to the antigen-bound acceptor dye occur. Steady-state and time-resolved fluorescence measurements reveal that approximately 50% of the donor quenching is due to RET, while the residual quenching effect is caused by the static quenching process.

KEY WORDS: Cyanine dyes; energy transfer; electron transfer; Poisson distribution.

INTRODUCTION

The most serious limitation of homogeneous fluoroimmunoassays (FIA) to widespread application is their inferior sensitivity compared to the equivalent heterogeneous methodology. These problems are caused mainly by interferences from sample accompanying substances and by high background signals from the sample matrices, which results in small changes of fluorescence intensity during the immunoreaction [1]. The background intensity is caused mainly by fluorescing compounds, such as proteins, which, in addition, contribute to the light scattering by the sample (Rayleigh and Raman scattering) [2]. However, the limitation of high background fluorescence can be overcome by using red-absorbing fluorophores, such as oxazines [3,4], thiazines [5], or cyanines [6–11], thus also taking advantage of reduced light scattering at longer wavelengths and minimal tissue absorbance particularly above 600 nm [12]. Because of their favorable spectroscopic properties, i.e., absorption bands between 600 and 900 nm and large extinction coefficients (130,000–250,000 $M^{-1} \cdot cm^{-1}$), and acceptable fluorescence quantum yields ($\phi_F > 0.2$), cyanine dyes have already been successfully employed as fluorescent labels in FIA-based applications [13–15].

This paper describes the use of two sulfoindocyanine dyes, Cy5 [6] and Cy5.5 [7] (for chemical structures see Fig. 1), for the development of a homogeneous FIA based on energy transfer. For this purpose antibodies were labeled with Cy5 (donor), while a tracer was synthesized

[1] Institute of Physical and Theoretical Chemistry, Auf der Morgenstelle 8, D-72076 Tübingen, Germany.
[2] DC-LCPPM, EPFL, CH-1014 Lausanne-Ecublens, Switzerland.
[3] To whom correspondence should be addressed. Fax: [49] (7071) 295490. e-mail: Guenter.Gauglitz@ipc.uni-tuebingen.de

1053-0509/00/0600-0147$18.00/0

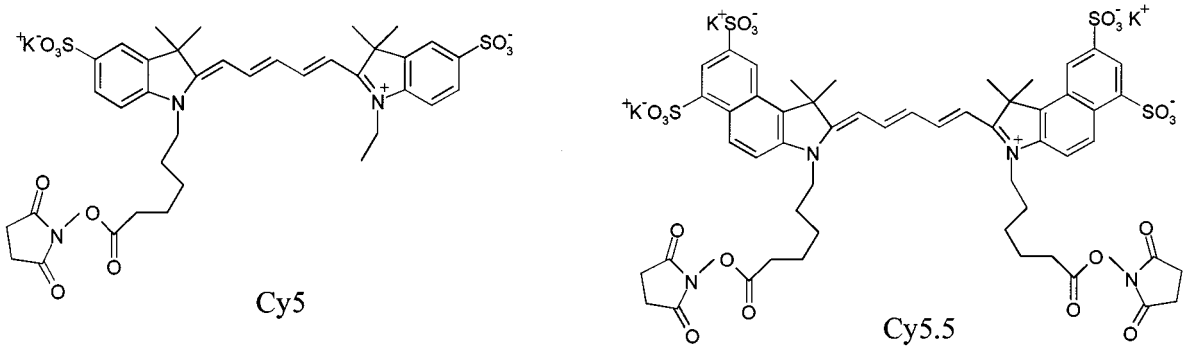

Fig. 1. Chemical structures of the sulfoindocyanine dyes Cy5 and Cy5.5 used in this investigation.

by coupling Cy5.5 (acceptor) and an analyte derivative subsequently to bovine serum albumin (BSA). Since cyanine dyes are known to form nonfluorescent aggregates (dimer formation) [16,17], particularly when present at high concentrations on protein surfaces, an accurate adjustment of the labeling ratio is indispensable. Especially The dye/protein ratio of the donor is of crucial importance for high signal dynamics upon formation of the antibody–antigen complex, when the decrease in the donor fluorescence intensity is monitored. Therefore a detailed investigation of the effect of dimer formation on the fluorescence quantum yield of the antibody bound Cy5 is performed and described quantitatively. The energy transfer process in the antibody–antigen complex is investigated and the contribution of different photophysical processes to the deactivation of the primarily excited donor dye is elucidated.

EXPERIMENTAL PROCEDURES

Materials

N-Hydroxysuccinimidyl (NHS) esters of Cy5 (monofunctional) and Cy5.5 (bisfunctional) were purchased from Amersham Life Science, Braunschweig, Germany. The triazine derivative 4-chloro-6-(isopropylamino)-1,3,5-triazine-2-(6′-amino)caproic acid (atrazine caproic acid; ACA) was synthesized and purified as described in Ref. 18. Polyclonal antisimazine antibody (IgG) was received as a present from Dr. Ram Abuknesha, GEC, London. Solvents of analytical grade, Sephadex G-25 columns, and all other common chemicals and biochemicals were purchased from Sigma Chemical Co. (Deisenhofen, Germany) and Fluka (Neu-Ulm, Germany).

*Preparation of ACA–*N*-Hydroxysuccinimide Ester.* Three and seventy-six-hundredths milligrams (18 μmol) of dicyclohexylcarbodiimide (DCC) was added to a solution of 5 mg (16.5 μmol) of ACA and 2.1 mg (18 μmol) of *N*-hydroxysuccinimide (NHS) in 200 μl of absolute *N,N*-dimethylformamide (DMF) kept on ice. The mixture was stirred for 6 h at room temperature, filtered, and then used directly (without further purification) for conjugation to proteins.

Labeling of IgG and BSA with the Dyes. Twenty microliters of reactive dye (for molar ratios see Table I) in absolute DMF was added to a solution of 500 μg of protein (3.3 nmol IgG or 7.2 nmol BSA) in 250 μl of 0.1 *M* sodium carbonate-bicarbonate buffer, pH 9.7, and mixed thoroughly by gentle vortexing. The reaction was incubated at room temperature for 30 min. Unconjugated dye was separated from protein–dye conjugate by gel-permeation chromatography over Sephadex G-25 using phosphate-buffered saline (PBS; 10 m*M* potassium dihydrogenphosphate, 150 m*M* sodium chloride, pH 7.4) as eluent. The dye-to-protein ratio was determined spectrophotometrically by measuring the absorbance at 15,300 cm^{-1} (Cy5) or 14,700 cm^{-1} (Cy5.5) and 36,000 cm^{-1} (protein) in PBS:DMF (1:1, v/v) [11] and inserting the measured values into the equation

Table I. Molar Ratio of Reactive Dye and Protein Used in the Labeling Procedure in Comparison with the Obtained Dye/Protein Ratio of the Conjugates

Protein	Reactive dye	[Reactive dye]/[protein] ratio	[Attached dye]/[protein] ratio
IgG	Cy5–NHS	5	0.8
IgG	Cy5–NHS	20	3.7
IgG	Cy5–NHS	25	4.5
IgG	Cy5–NHS	35	8.7
BSA	Cy5.5–NHS	10	1.6
BSA	Cy5.5–NHS	20	2.9

$$[\text{attached dye}]/[\text{protein}] = \frac{A_{\text{dye}}\,\varepsilon_{\text{protein}}}{(A_{36{,}000} - XA_{\text{dye}})\varepsilon_{\text{dye}}} \quad (1)$$

The molar extinction coefficients of Cy5 and Cy5.5 (ε_{dye}) were assumed to be equal to their values in PBS (ε = 250,000 $M^{-1} \cdot \text{cm}^{-1}$ and ϵ = 190,000 $M^{-1} \cdot \text{cm}^{-1}$ respectively) and the extinction coefficients of IgG and BSA ($\varepsilon_{\text{protein}}$) were taken to be 201,700 $M^{-1} \cdot \text{cm}^{-1}$ and 45,540 $M^{-1} \cdot \text{cm}^{-1}$ respectively. The factor X in the denominator accounts for dye absorption at 36,000 cm^{-1}, which is 5 and 13% of the absorption of Cy5 [6] and Cy5.5 [7] at their maximum absorption (A_{dye}). The dye/protein ratios obtained are given in Table I.

Labeling of the BSA–Cy5.5 (1:1.6) Conjugate with ACA–NHS. A solution of 45 μg (150 nmol) of ACA–NHS in absolute DMF was added to a solution of 400 μg (5.8 nmol) of BSA–Cy5.5 conjugate in 250 μl of 0.1 *M* sodium carbonate–bicarbonate buffer, pH 9.7, and mixed thoroughly by gentle vortexing. The reaction condition and duration as well as the purification of the conjugate were the same as described above. The ACA concentration of the conjugates was determined by means of reflectometric interference spectroscopy (RIfS) [19]. The ACA/BSA ratio was found to be 3.6:1, corresponding to a labeling efficiency of 15%.

Resonance Energy Transfer (RET) Immunoassay. The principle of the RET immunoassay is illustrated in Fig. 2. The antibody (antisimazine) was labeled with the donor Cy5 (IgG–Cy5). An analyte derivative (ACA) and the acceptor Cy5.5 were subsequently coupled to bovine serum albumin (BSA), which served as the carrier molecule (ACA–BSA–Cy5.5). The assay was performed by adding 50 μl of ACA–BSA–Cy5.5 conjugate to 450 μl of IgG–Cy5 conjugate. The conjugates were dissolved in PBS, pH 7.4, containing 100 μg/ml chicken egg albumin (OVA) as background protein. After addition of the ACA–BSA–Cy5.5 conjugate the solution was incubated for 10 min at 20°C. After equilibration, the fluorescence intensity was measured at 15,000 cm^{-1}.

Methods

Absorption spectra were recorded on a Perkin–Elmer λ2 spectrophotometer. Fluorescence excitation and emission spectra were obtained with a Perkin–Elmer LS-50 B luminescence spectrometer equipped with a red-sensitive photomultiplier R928. Polarization spectra and anisotropies were determined using a Spex Fluorolog 222 spectrofluorometer. Fluorescence lifetimes were determined with a Spex Fluorolog 112, applying the single-photon counting technique using equipment from EG&G ORTEC. The light source was a Hamamatsu laser diode at 15,300cm^{-1}. The emission was detected through a 14,900-cm^{-1} cutoff filter. The emission monochromator was set to 14,700 and 14,200 cm^{-1} for recording the decays of Cy5 and Cy5.5, respectively.

Fluorescence Lifetime and Quantum Yield. Time-resolved decays of fluorescence intensities $I(t)$ were fitted as a sum of exponentials,

$$I(t) = \sum_i \alpha_i e^{-t/\tau_i} \quad (2)$$

where τ_i is the decay time and α_i the corresponding preexponential factor. The parameters τ_i and α_i were determined using least-squares analysis software. Equation (2) was also used for fitting time-resolved fluorescence decays of protein-bound dyes which are additionally deactivated by RET, assuming that donor and acceptor are separated by a fixed distance rather than being distributed randomly. This situation is frequently encountered for labeled proteins [20].

The mean lifetime $\bar{\tau}$ was calculated according to

$$\bar{\tau} = \sum_i \alpha_i \tau_i^2 / \sum_i \alpha_i \tau_i \quad (3)$$

The fluorescence quantum yields ϕ_F(conjugate) of Cy5 monomers in the IgG–Cy5 conjugate (1:3.7) and of Cy5.5 monomers in the BSA–Cy5.5 conjugate (1:1.6) were determined according to

$$\phi_F(\text{conjugate}) = \phi_F(\text{dye}) \frac{\tau_F(\text{conjugate})}{\tau_F(\text{dye})} \quad (4)$$

where ϕ_F(dye) is the fluorescence quantum yield of the free dye in solution and τ_F(conjugate) and τ_F(dye) are the experimental fluorescence lifetimes of the conjugate and of the corresponding dye, respectively.

The quantum yields of the IgG–Cy5 conjugates (1:0.8, 1:4.5, and 1:8.7) and of the BSA–Cy5.5 conjugate

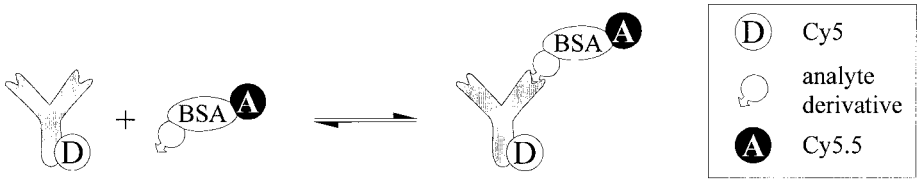

Fig. 2. Schematic description of the RET immunoassay.

(1:2.9) were determined relative to the fluorescence quantum yields of the conjugates determined above, by correcting the contribution of nonfluorescent dimeric species to the absorbance at the excitation wavenumber 15,400 cm^{-1} and calculating the area under the corrected emission spectra. The experimental errors in fluorescence lifetime and quantum yield measurements are ca. ±5%.

Förster Distance. The Förster distance R_0 [21] was calculated using

$$R_0^6 = \frac{9000(\ln)\kappa^2\phi_D J}{128\pi^5 n^4 N_{AV}} \quad (5)$$

where κ^2 is the orientation factor, ϕ_D is the donor quantum yield in the absence of acceptor molecules, J is the overlap integral, n is the refractive index of the medium, and N_{AV} is Avogadro's number. For the orientation factor κ^2 the average value of $^2/_3$ for randomly oriented donors and acceptors in solution was assumed. The index of refraction n in PBS was assumed to be 1.33.

RESULTS AND DISCUSSION

Spectral Properties

Absorption and fluorescence spectra of the two dyes in PBS are shown in Fig. 3. The absorption maximum of Cy5 and Cy5.5 in PBS are at $\tilde{\nu}$ = 15,500 cm^{-1} and $\tilde{\nu}$ = 14,800 cm^{-1}, respectively; the emission maxima are Stokes-shifted by ca. 420 and 360 cm^{-1}, respectively. Binding of the dyes to the proteins leads to shifts of the absorption maxima to lower wavenumbers by ca. 50 cm^{-1} for Cy5 and 110 cm^{-1} for Cy5.5, reflecting a higher polarisability of the environment. Fluorescence maxima are shifted by 50 and 210 cm^{-1}, respectively.

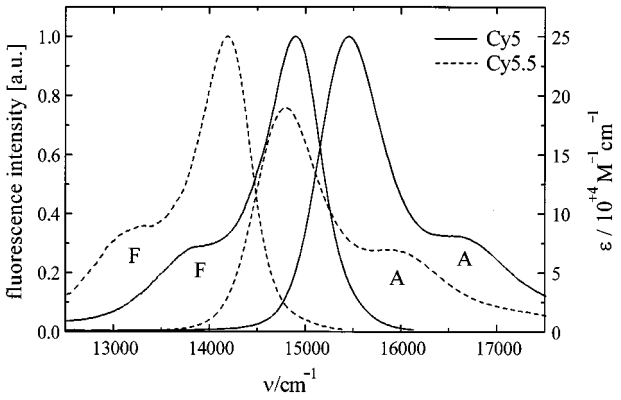

Fig. 3. Absorption (A) and fluorescence (F) spectra of Cy5 (——) and Cy5.5 (---), both 1 × 10^{-6} *M* in PBS.

With increasing labeling ratios a drastic change in the absorption properties of the dyes is observed. Figure 4 illustrates the spectral changes for the prepared IgG–Cy5 conjugates. The strongest band in the excitation spectrum becomes weaker as the dye/protein ratio increases, and a new band appears at longer wavenumbers (16,500 cm^{-1}). This is due to excitonic interaction between the obliquely oriented transition dipole moments of two Cy5 molecules forming a physical dimer [22,23].

Similar curves have been found for the BSA–Cy5.5 conjugates discussed in this paper. The spectra of the dimers, depicted in Fig. 4 for the antibody bound Cy5, were calculated as described in a previous study [24], following the method proposed by Förster and König [25]. Since the fluorescence excitation spectra of the conjugates are superimposable on the monomer absorption spectra, it can be concluded that the dimers are essentially nonfluorescent.

Quantum Yields

Using the fluorescence excitation spectra and the absorption spectra of the dimers, the proportions of monomers and dimers on each protein conjugate are calculated. Table II lists the values obtained. With the knowledge of the monomer/dimer ratio, it was possible to determine the quantum yields, ϕ_F^m, of the protein-bound monomeric dyes. The increase in ϕ_F^m at low dye/protein ratios (see Table II) is due to the restricted torsional motion about the central methine bridge [26]. At higher dye/protein ratios a drastic decrease in ϕ_F^m is obtained, which is caused by RET from monomeric dyes to increasing numbers of physical dimers on the proteins.

In the following a model is presented which quantitatively describes the dependence of ϕ_F^m on the labeling

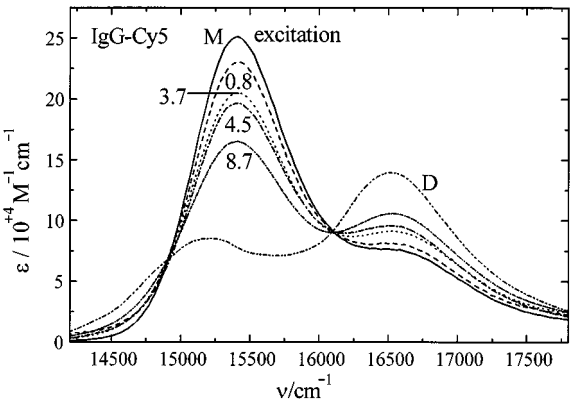

Fig. 4. Absorption spectra of IgG–Cy5 with various dye/protein ratios in PBS solution and calculated spectrum of pure dimer (D). The monomer absorption spectrum (M) is superimposable on the fluorescence excitation spectra of these conjugates.

Table II. Percentage of Monomer Dye Molecules Present on the Proteins and the Resultant Association Constants; Quantum Yields of Free and Protein-Bound Monomeric Cy5 and Cy5.5 Are Given in the Last Column

	Monomer (%)	K	ϕ_P[a]
Cy5	100	—	0.27[b]
IgG–Cy5 (0.8)	90	0.08	0.88
IgG–Cy5 (3.7)	74	0.06	0.44
IgG–Cy5 (4.5)	69	0.07	0.40
IgG–Cy5 (8.7)	52	0.10	0.14
Cy5.5	100	—	0.23[c]
BSA–Cy5.5 (1.6)	84	0.07	0.36
BSA–Cy5.5 (2.9)	76	0.07	0.21

[a] Phosphate-buffered saline (PBS).
[b] Value from Ref. 6.
[c] Value from Ref. 7.

ratio. It is assumed that energy transfer takes place between donors and acceptors which are attached at a single fixed distance to the same protein molecule. The distribution of both monomers and dimers among the protein molecules is described by Poisson statistics.

Quantum Yield. The fluorescence intensity (I_F) of the monomeric dyes at a mean labeling ratio of μ, in the absence of RET processes, is given by

$$I_F = I_{abs}\phi_F^m = I_{abs} \cdot \frac{\phi_{F,\mu\to 0}^m \, \varepsilon^m c^m}{\varepsilon^m c^m + \varepsilon^d c^d} \tag{6}$$

where I_{abs} is the intensity of the absorbed light, $\phi_{F,\mu\to 0}^m$ is the fluorescence quantum yield of the monomers at infinitely low labeling ratios, ε^m and ε^d are the extinction coefficients of the monomers and dimers, respectively, at the excitation wavenumber, and c^m and c^d are the concentrations of the monomers and dimers, respectively. In the presence of RET processes the fluorescence quantum yield ϕ_F^m is calculated by

$$\phi_F^m = \frac{\phi_{F,\mu\to 0}^m \varepsilon^m c^m}{\varepsilon^m c^m + \varepsilon^d c^d} \cdot (1 - \overline{E}) \tag{7}$$

where $\overline{E}$ is the mean RET efficiency. The calculation of $\overline{E}$ can be performed according to the following procedure.

Distribution of the Dyes. If μ is the average number of dyes bound per protein (labeling ratio), the probability of finding a protein with N_μ dyes is given by the Poisson distribution

$$P(N_\mu, \mu) = \frac{\mu^{N_\mu}}{N_\mu!} e^{-\mu} \tag{8}$$

The dyes associate to dimers according to the law of mass action, which is presumed still to be valid in the heterogeneous environment of the system considered. Thus, the mean number of dimers δ at a given value of N_μ is calculated by

$$\delta = \frac{(4KN_\mu + 1) - \sqrt{(4KN_\mu + 1)^2 - 16K^2N_\mu^2}}{8K} \tag{9}$$

where K is the association constant of the monomer $\rightleftharpoons$ dimer equilibrium on a single protein. Analogous to Eq. (8), the probability $[P(D_\delta, \delta)]$ of finding a protein with D_δ dimers at a given mean number of δ dimers per protein is expressed by the Poisson distribution.

Transfer Efficiency. From the equations developed by Förster [27], the rate of energy transfer k_{RET} between two point dipoles at a distance R is

$$k_{RET} = \frac{1}{\tau_F}\left(\frac{R_0}{R}\right)^6 \tag{10}$$

where R_0 is the distance at which k_{RET} equals the deactivation rate ($1/\tau_F$) in the absence of quencher. For a single donor molecule attached on a protein beating D_δ dimers, the rate of energy transfer is the sum of the individual rates $k_{RET,i}$ of transfer to each dimer. Following an analysis similar to that of Gennis and Cantor [28], the transfer efficiency is given by

$$E(D_\delta) = \frac{\tau_F \sum_{i=1}^{D_\delta} k_{RET,i}}{1 + \tau_F \sum_{i=1}^{D_\delta} k_{RET,i}} \tag{11}$$

Making the simplifying assumption that all the dimers are localized at a mean distance $\overline{R}$ from the donor molecule, $E(M_\mu, D_\delta)$ for a single protein molecule bearing $M_\mu = N_\mu - 2D_\delta$ monomers and D_δ dimers is given by

$$E(M_\mu, D_\delta) = (N_\mu - 2D_\delta)\frac{D_\delta(R_0/\overline{R})^6}{1 + D_\delta(R_0/\overline{R})^6} \tag{12}$$

According to the treatment of Gennis and Cantor, the mean transfer efficiency is the weighted average of the $E(M_\mu, D_\delta)$, where the weighting factors are the Poisson terms discussed above. Hence

$$\overline{E} = \sum_{N_\mu=0}^{n} \frac{1}{N_\mu} \sum_{D\mu=0}^{m} \{P(N_\mu, \mu) \cdot P(D_\delta, \delta) \cdot E(M_\mu, D_\delta)\} \tag{13}$$

where n and m are the points at which the series are truncated and are arbitrarily taken as values large enough to avoid significantly affected numerical results.

Calculation of the Parameters. By combining Eqs. (7) and (13) the fluorescence quantum yield ϕ_F^m of the

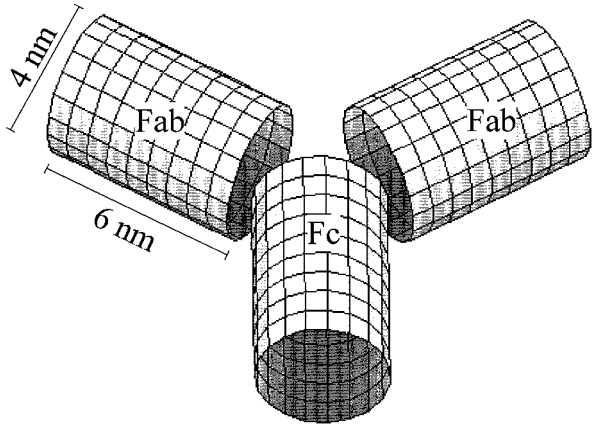

Fig. 5. Presentation of the antibody model used for the calculation of $\bar{R}$.

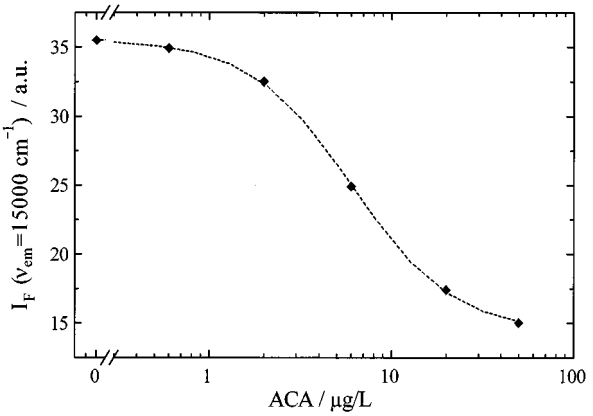

Fig. 7. Quenching of Cy5 fluorescence upon titration of 10 μg/ml IgG–Cy5 with increasing concentrations of ACA–BSA–Cy5.5 (0–50 μg/L).

monomeric dyes in the presence of RET processes to dimers can be calculated as a function of μ, $\phi^{m}_{F,\mu\to0}$, R_0, K, and $\bar{R}$.

Inserting in to Eq. (5) a fluorescence quantum yield of $\phi^{m}_{F,\mu\to0} = 1$ for the donor and an extinction coefficient of $\varepsilon_{16500} = 279{,}000\ M^{-1}\,\mathrm{cm}^{-1}$ for the acceptor, the Förster distance R_0 for energy transfer from monomeric Cy5 to Cy5 dimers is obtained as $R_0 = 8.39$ nm. The association constant of the monomer ⇌ dimer equilibrium can be derived from the proportion of monomers and dimers on each protein conjugate (see Table II) and equals $K = 0.08 \pm 0.02$ for Cy5. The mean distance $\bar{R}$ between randomly attached donor and acceptor molecules was calculated to be 5.9 nm, assuming an antibody geometry consisting of three equivalent cylindrical fragments with the dimensions given in Fig. 5.

Comparison of Calculated and Experimental Values. In Fig. 6 the calculated fluorescence quantum yields are compared with the experimental values given in Table II. Considering the simplicity of the model, a fairly good agreement between experimental and calculated values is achieved. From this the fluorescence quantum yield of the monomeric Cy5 in absence of dimers can be determined to be close to unity. Thus, the restriction of the Cy5 molecule to a planar conformation through covalent binding of the heteroaromatic fragment to the antibody reduces dramatically the rate of the internal conversion process [26,30,31].

The maximum of fluorescence intensity per labeled antibody can be derived by multiplying the fluorescence quantum yield of Cy5 monomer with the number of monomeric Cy5 on the antibody. With rising CyS/IgG

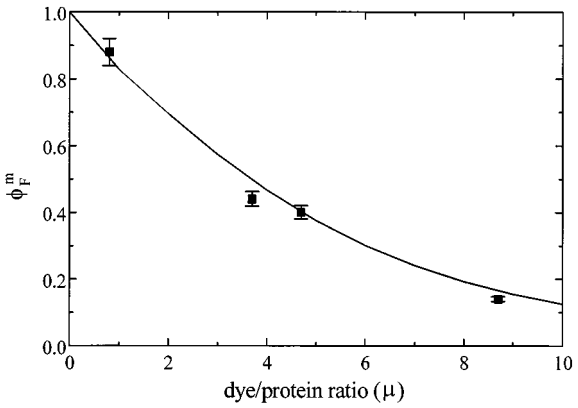

Fig. 6. Dye/protein ratio μ versus ϕ^{m}_{F} for antibody-bound Cy5. The solid line represents the calculated values using $\phi^{m}_{F,\mu\to0} = 1$, $R_0 = 8.39$ nm, $K = 0.1\ M^{-1}$, and $R = 5.9$ nm.

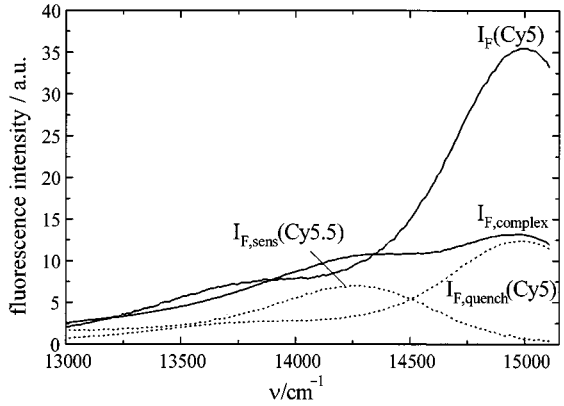

Fig. 8. Fluorescence spectra of 10 μg/ml IgG–Cy5 in the absence [I_F(Cy5)] and in the presence of 50 μg/L ACA–BSA–Cy5.5 [$I_{F,quench}$(Cy5)]. The spectrum of $I_{F,complex}$ has been corrected for the contribution of direct excited Cy5.5 fluorescence. The dotted lines are fits of IgG–Cy5 [$I_{F,quench}$(Cy5)] and ACA–BSA–Cy5.5 [$I_{F,sens}$(Cy5.5)] spectra to $I_{F,complex}$ and represent the fluorescence intensity of the unquenched IgG–Cy5 and sensitized ACA–BSA–Cy5.5, respectively.

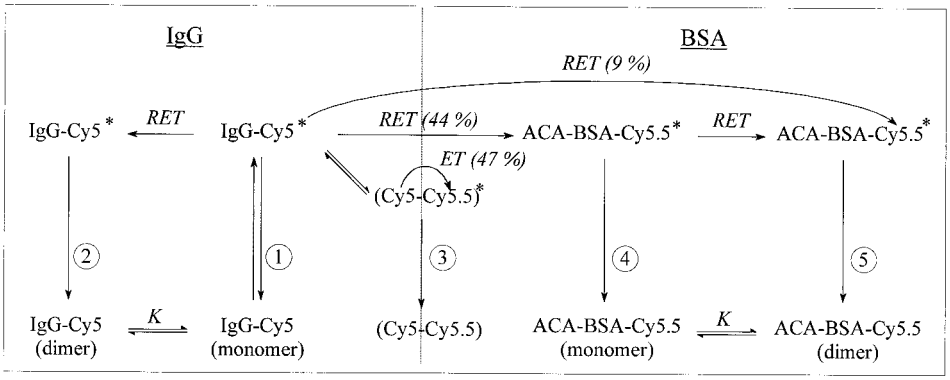

Fig. 9. Deactivation scheme of excited antibody-bound monomeric Cy5. (1) Fluorescence of monomeric Cy5; (2) nonradiative deactivation of dimeric Cy5; (3) static quenching by electron transfer (ET); (4) sensitized fluorescence of monomeric Cy5.5; (5) nonradiative deactivation of dimeric Cy5.5.

ratios the fluorescence increases, reaching a maximum at a Cy5/IgG ratio of approximately 4. At higher Cy5/IgG ratios fluorescence quenching by RET begins to dominate, resulting in decreasing fluorescence intensity. This result is in good agreement with the value obtained in an earlier report [9] for a similar carboxymethylindocyanine dye (Cy5.12).

Energy Transfer in the Antibody–Antigen Complex

Addition of increasing amounts of ACA–BSA–Cy5.5 (3.6:1:1.6) to a fixed concentration of IgG–Cy5 (1:3.7) (10 μg/ml) produced decreases in the fluorescence intensity which approached a minimum value with 50 μg/L ACA (Fig. 7).

The total quenching of the IgG–Cy5 fluorescence can be calculated as the difference of the fluorescence intensities of IgG–Cy5 in the absence [I_F(Cy5)] and in the presence of 50 μg/L ACA–BSA–Cy5.5 [$I_{F,quench}$(Cy5)[. For this the measured emission spectra of the antibody–antigen complex, ($I_{F,complex}$) has to be represented as a linear combination of $I_{F,quench}$(Cy5) and the sensitized ACA–BSA–Cy5.5 fluorescence [$I_{F,sens}$ (Cy5.5)] as shown in Fig. 8. Thus, the total quenching equals 0.65.

Quenching by RET. The fraction of fluorescence intensity of IgG–Cy5 which is quenched due to RET from Cy5 to Cy5.5 and thus leads to the sensitized fluorescence of Cy5.5, $I_{F,sens}$(Cy5.5), equals 0.34 (corresponding to 53% of the total quenching). The same result is obtained by measuring the fluorescence lifetimes of IgG–Cy5. A decrease in the mean fluorescence lifetimes of Cy5 in the antibody–antigen complex from 1.54 to 1.06 ns is obeserved, as is expected for the dynamic RET process. From this it follows that a fraction of 0.31 (corresponding to 48% of the total quenching) of the donor excitation energy is deactivated by RET. This slight discrepancy between the fraction of fluorescence quenching by RET, which is derived from the steady-state (0.34) and the lifetime (0.31) measurements, is within experimental error. Using the data from Table II the fraction of RET from IgG–Cy5 to the BSA-bound Cy5.5 monomers and dimers can be calculated as 0.28 (44%) and 0.06 (9%), respectively (see Fig. 9).

Quenching by Electron Transfer (E.T). The fraction of the IgG–Cy5 quenching which could not be ascribed to RET processes (47% of the total quenching) must be assigned to static quenching (see Fig. 9). The most likely mechanism responsible for this static quenching is the deactivation of the excitation energy of Cy5 by ET to adjacent Cy5.5 molecules. ET as the deactivation channel for excited cyanine dyes is a well-known photophysical property of cyanine dyes and is described extensively in the literature [32,33]. The occurrence of ET as a competing process with RET has already been pointed out by West [36].

ACKNOWLEDGMENTS

This work was supported by the German Ministry of Education, Science, Research and Technology under the "Mikrosystemtechnik 1994–1998" program (project LINDAU/16SV541/VDI-VDE IT) and by the DFG (Forschergruppe "Molekulare Mustererkennung. . ." and Graduiertenkolleg "Quantitative Analyse und Charakterisierung pharmazeutisch und biochemisch relevanter Substanzen" at the University of Tübingen).

REFERENCES

1. I. Hemmilä (1985) *Clin. Chem.* **31**, 359–370.
2. E. Soini and I. Hemmilä (1979) *Clin. Chem.* **25**, 353–361.
3. S. Hassoon and I. Schechter (1998) *Anal. Chim. Acta* **368**, 77–82.
4. M. P. Aguilar-Caballos, A. Gómez-Hens, and D. Pérez-Bendito (1999) *Anal. Chim. Acta* **381**, 147–154.
5. T. Imasaka, A. Tsukamoto, and N. Ishibashi (1989) *Anal. Chem.* **61**, 2285–2288.
6. R. B. Mujumdar, L. A. Ernst, S. R. Mujumdar, C. J. Lewis, and A. S. Waggoner (1993) *Bioconj. Chem.* **4**, 105–111.
7. S. R. Mujumdar, R. B. Mujumdar, C. M. Grant, and A. S. Waggoner (1996) *Bioconj. Chem.* **7**, 356–362.
8. L. A. Ernst, R. K. Gupta, R. B. Mujumdar, and A. S. Waggoner (1989) *Cytometry* **10**, 3–10.
9. P. L. Southwick, L. A. Ernst, E. W. Tauriello, S. R. Parker, R. B. Mujumdar, S. R. Mujumdar, H. A. Clever, and A. S. Waggoner (1990) *Cytometry* **11**, 418–430.
10. N. Narayanan, L. Strekowski, M. Lipowska, and G. Patonay (1995) *J. Org. Chem.* **60**, 2391–2395.
11. E. Terpetschnig, H. Szmacinski, A. Ozinskas, and J. R. Lakowicz (1994) *Anal. Biochem.* **217**, 197–204.
12. C. Cullander (1994) *J. Microsc.* **176**, 281–286.
13. R. J. Williams, J. M. Peralta, V. C. W. Tsang, N. Narayanan, G. A. Casay, M. Lipowska, L. Strekowski, and G. Patonay (1997) *Appl. Spectrosc.* **51**, 836–843.
14. R. M. Wadkins, J. P. Golden, L. M. Pritsiolas, and F. S. Ligler (1998) *Biosens. Bioelectron.* **13**, 407–415.
15. A. Klotz, A. Brecht, C. Barzen, G. Gauglitz, R. D. Harris, G. R. Quigley, J. S. Wilkinson, and R. A. Abuknesha (1998) *Sens. Act. B* **51**, 181–187.
16. Q. Li and B. X. Peng (1998) *Dyes Pigment* **36**, 323–337.
17. A. Sidorowicz, A. Pola, and P. Dobryszycki (1997) *J. Photochem. Photobiol. B* **38**, 94–97.
18. M. Weller (1992) *Strukturelle und kinetische Untersuchungen zur Entwicklung und Optimierung von Hapten-Enzymimmunoassays (ELISAs) am Beispiel der Bestimmung von Triazinherbiziden*, Dissertation TU München, Fakultät für Chemie, Biologie und Geowissenschaften.
19. J. Piehler, A. Brecht, T. Giersch, B. Hock, and G. Gauglitz (1997) *J. Immunol. Methods* **201**, 189–206.
20. J. R. Lakowicz (1983) *Principles of Fluorescence Spectroscopy*, Plenum Press, New York.
21. B. W. Van Der Meer, G. Coker III, and S.-Y. S. Chen (1994) *Resonance Energy Transfer—Theory and Data*, Verlag Chemie, Weinheim.
22. W. West and S. Pearce (1965) *J. Phys. Chem.* **69**, 1894–1903.
23. F. Nüesch and M. Grätzel (1995) *Chem. Phys.* **193**, 1–17.
24. U. Schobel, H.-J. Egelhaaf, A. Brecht, D. Oelkrug, and G. Gauglitz (1999) *Bioconj. Chem.* (in press).
25. T. Förster and E. König (1957) *Z. Elektrochem.* **61**, 344–348.
26. T. L. Netzel, K. Nafisi, M. Zhao, J. R. Lenhard, and I. Johnson (1995) *J. Phys. Chem.* **99**, 17936–17947.
27. T. Förster (1948) *Ann. Phys.* **2**, 55–75.
28. R. B. Gennis and C. R. Cantor (1972) *Biochemistry* **11**, 2509–2517.
29. L. P. Southwick, L. A. Ernst, E. W. Tauriello, S. R. Parker, R. B. Mujumdar, S. R. Mujumdar, H. A. Clever, and A. S. Waggoner (1990) *Cytometry* **11**, 418–430.
30. C. J. Tredwell and C. M. Keary (1979) *Chem. Phys.* **43**, 307–316.
31. C. Carlsson, A. Larsson, M. Jonsson, B. Albinsson, and B. Nordén (1994) *J. Chem. Phys.* **98**, 10313–10321.
32. D. Doizi and J. C. Mialocq (1987) *J. Phys. Chem.* **91**, 3524–3530.
33. H. Killesreiter (1979) *Z. Naturforsch.* **34a**, 737–747.
34. R. Bauer and C. Königstein (1993) *Z. Natruforsch.* **48b**, 461–470.
35. K.-H. Feller and R. Gadonas (1996) *AIP Conf. Proc.* **364**, 78–90.
36. W. West (1970) in W. F. Berg, U. Mazzucato, H. Meier, and G. Semerano (Eds.), *Dye Sensitization*, Focal Press, London, p. 105.